Journal of Colloid and Interface Science 384 (2012) 137–142

Contents lists available at SciVerse ScienceDirect

Journal of Colloid and Interface Science

www.elsevier.com/locate/jcis

Highly-controlled grafting of mono and dicationic 4,4′-bipyridine derivatives on SBA-15 for potential application as adsorbent of $CuCl_2$ from ethanol solution

Natalia Fattori [a], Camila M. Maroneze [a], Herica A. Magosso [b], Yuriy V. Kholin [c], Yoshitaka Gushikem [a,*]

[a] Institute of Chemistry, State University of Campinas, PO Box 6154, 13083-970 Campinas, SP, Brazil
[b] Department of Chemistry, Federal University of Santa Catarina, PO Box 476, 88040-900 Florianópolis, SC, Brazil
[c] Materials Chemistry Department, V.N. Karazin Kharkiv National University, 4 Svoboda Square, 61022 Kharkiv, Ukraine

ARTICLE INFO

Article history:
Received 19 April 2012
Accepted 20 June 2012
Available online 4 July 2012

Keywords:
SBA-15
4,4′-Bipyridine
Adsorbents
Anionic copper complex
Functional surface monolayer

ABSTRACT

This work describes a highly controlled post-grafting of mono and dicationic 4,4′-bipyridine alkoxysilane derivatives ($Bipy^+$ and $Bipy^{2+}$) onto the surface of an ordered mesoporous silica, SBA-15. The materials obtained are designated as SBA-15/$Bipy^+Cl^-$ and SBA-15/$Bipy^{2+}Cl_2^-$, both possessing chloride as counter ion. The regular arrangement of uniform pores of this inorganic matrix is likely to ensure good accessibility to the active centers (electron acceptors) attached to the surface. The materials are excellent adsorbents due to the ability of the functional groups to retain copper chlorides on their surfaces as anionic complexes ($CuCl_{2+n}^{n-}$) in ethanol. From the adsorption results it was possible to probe the functional surface monolayer of the materials, which present a highly homogenous distribution of functional groups inside the ordered SBA-15 channels, with an exchange efficiency of 93% for SBA-15/$Bipy^+Cl^-$ and 94% for SBA-15/$Bipy^{2+}Cl_2^-$. Both adsorbent materials are potentially useful in the pre-concentration and further analysis of Cu(II) present in trace amounts in ethanol, extensively used as an automotive fuel in Brazil.

1. Introduction

Organically functionalized mesoporous silicas have proven to be particularly attractive due to the possibility to combine a diversity of functional organic properties with the advantages of a thermally stable and robust inorganic substrate. The synergism between organic and inorganic components can result in materials whose properties differ considerably from those of their individual components.

The most common functionalization procedure is the post-grafting synthesis, where a silane containing the desired functional group is directly attached to the surface, providing the resulting materials differentiated physical and chemical properties and making them suitable for catalysis [1–4], enzyme immobilization [5,6], controlled release of biological molecules [7], modified electrodes [8], and the adsorption of metal ions and organic molecules [9–15].

Considerable efforts have been done to develop new adsorbents for removing metal ions and other toxic species from water and non aqueous solvents [15–18]. The use of modified mesoporous silica for these purposes is advantageous since their pore sizes are large enough to accommodate functional organic groups and to facilitate the diffusion of the solvated species, providing a unique environment for chemical separations and reactions.

Surface modifications with organic functionalities such as C–C multiple bonds, thiols, sulfonic and carboxylic acids, and amines have been widely used, and allow, for example, localized reactions to be carried out on stable solid inorganic matrices [19–23]. Among several different functional groups reported in the literature, there is considerable interest in the use of 4,4′-bipyridine derivatives to modify the surface of mesoporous silicas because of their interesting and well-known electron acceptor, charge transfer and fluorescence properties [24–26]. The quaternary salts of 4,4′-bipyridine, commonly known as viologen, are widely used as anion exchange groups in membranes [27], thermosensors [28], colorimetric sensors [29], for photocatalytic hydrogen evolution [30], for the design of optical materials [31] and for fluorescence probing [32]. The 4,4′-bipyridinium cations have a relatively high electron affinity and therefore readily form charge-transfer complexes with electron rich species (anions). With non-interacting counter-ions, quaternary bipyridinium salts are colorless, but with strongly interacting ions, a charge transfer interaction occurs to give strongly colored solids [26].

In the present study, the interest in mesoporous silicas modified with 4,4′-bipyridine derivatives is based on the fact that these materials can be used to adsorb metal anionic complexes. The immobilization of metallic complexes on the surface of modified silicas plays a very important role in many areas of chemistry, such

* Corresponding author. Fax: +55 19 35213023.
E-mail address: gushikem@iqm.unicamp.br (Y. Gushikem).

0021-9797/$ - see front matter © 2012 Elsevier Inc. All rights reserved.
http://dx.doi.org/10.1016/j.jcis.2012.06.065

as heterogeneous catalysis, in the synthesis of supported metal nanoparticles, in the adsorption process of metal ions, and in the development of fluorescent devices [33–38]. Xu et al. prepared $ZnCl_3$(4-methyl-4,4′-bipyridinium) complexes with photoluminescent properties [39], and Yuan et al. reported the immobilization of $CuCl_2$ in mesoporous molecular sieves organofunctionalized with 3-aminopropyltrimethoxysilane for the catalytic carbonylation of methanol to produce dimethyl carbonate [33].

The present work describes the preparation and characterization of SBA-15 chemically modified by a post-grafting process with mono and dicationic derivatives of 4,4′-bipyridine, with highly uniform functional group distributions. The organic functional groups can interact with metal ions in ethanol solution, forming MCl_{2+n}^{n-} anionic complexes retained by electrostatic interaction with the fixed cationic groups. The effectiveness of the resulting materials as potential adsorbents for metal ions from ethanol was tested for $CuCl_2$, used as a probe.

Studies carried out on the adsorption process of MCl_z (M = Fe(III), Cu(II), Zn(II), Co(II), and Cd(II)) on the surface of non-ordered silicas by similar covalently bonded cationic functional groups are not so efficient, considering their non uniform distribution on the surface [40–42]. In a recent work, the efficiency of the post functionalized matrices with a bicationic 1,4-diazabicyclo[2.2.2]octane derivative on mesoporous ordered (SBA-15) and non-ordered (DMS) silica showed the effectiveness of the former matrix in retaining $CuCl_2$, in comparison with the second, due to the higher degree of dispersion of the functional groups on the surface of SBA-15 [43].

2. Materials and methods

2.1. Synthesis of mesoporous SBA-15

Mesoporous silica SBA-15 was prepared according to the following procedure, based on the method reported by Zhao et al. [44,45]. Tetraethylorthosilicate (TEOS, Acros, 98%) was used as the silica source, and Pluronic® P123 (M_{av} = 5800, $EO_{20}PO_{70}EO_{20}$, Aldrich) acted as the template to direct the formation of the well-ordered porous structure. 4.0 g of Pluronic® P123 was dissolved in 30.0 g of water and 120.0 g of 2.0 mol L^{-1} aqueous HCl solution. The temperature was increased to 313 K, and 8.5 g of TEOS was added. The mixture was stirred for 5 min. Afterward, the solution was allowed to stand for 20 h at 313 K. The mixture was then placed in an autoclave at 373 K for 24 h for hydrothermal treatment. After cooling to room temperature, the solid product was recovered, washed with bidistilled water, and dried at 373 K. Calcination of the solid obtained was carried out under an air flow, slowly increasing the temperature at a heating rate of 2 K min^{-1} from room temperature to 823 K. The solid was heated at 823 K for 6 h.

2.2. Synthesis of the silylating agents $Bipy^+I^-$ and $Bipy^{2+}I_2^-$

The silylating agents, $Bipy^+I^-$ and $Bipy^{2+}I_2^-$, were prepared based on a procedure described in the literature [30,46]. Briefly, to prepare (N-(trimethoxysilylpropyl)-4,4′-bipyridinium iodide ($Bipy^+I^-$), 0.030 mol of 4,4′-bipyridine (Aldrich) and 0.030 mol of 3-iodopropyltrimethoxysilane (IPTMS, Aldrich) were added to 60.0 mL of CH_3CN and the solution stirred for 48 h at 298 K under a nitrogen atmosphere. Then, the temperature was raised to 358 K and the solution was stirred for an additional 24 h. The orange solid obtained was filtered and washed with toluene. Finally, the resulting solid was heated at 353 K at 10^{-4} torr to eliminate all residual solvent. A similar procedure was used to prepare the (N′-N-bis(trimethoxysilylpropyl)-4,4′-bipyridinium diiodide ($Bipy^{2+}I_2^-$) by reacting 0.030 mol of 4,4′-bipyridine and 0.060 mol of IPTMS.

2.3. Surface functionalization of SBA-15 with the silylating agents

3.0 g of SBA-15 was immersed into aqueous solutions of $Bipy^+I^-$ or $Bipy^{2+}I_2^-$ (300 mL, 2.0×10^{-2} mol L^{-1}). The mixtures were allowed to remain at 298 K, under continuous stirring, for 24 h. The solids obtained were then filtered and exhaustively washed with bidistilled water. The modified materials are denominated as SBA-15/$Bipy^+I^-$ and SBA-15/$Bipy^{2+}I_2^-$.

Since our interest is to have Cl^- as the exchangeable counter ion and not I^-, the functionalized solids were immersed in 1.0 mol L^{-1} aqueous HCl, stirred for a few minutes, filtered and washed with 1.0×10^{-3} mol L^{-1} aqueous NH_4OH and bidistilled water, resulting in materials with Cl^- as counter ions, denominated as SBA-15/$Bipy^+Cl^-$ and SBA-15/$Bipy^{2+}Cl_2^-$.

2.4. Characterization

Scanning electronic microscopy (SEM) images were acquired on a JEOL JSM 6360LV scanning electron microscope, operating at 20 kV. The samples were fixed onto double-faced carbon tape and gold-coated using a Bal-Tec MD20 instrument. Transmission electron microscopy (TEM) images were obtained on a JEOL JEM 2100 HTP transmission electron microscope operating at 200 kV.

N_2 adsorption–desorption isotherms were measured at 77 K on a Quantachrome Autosorb 1 instrument. The samples were previously outgassed at 353 K for 6 h. The Brunauer–Emmett–Teller (BET) method was employed to calculate the specific surface areas (S_{BET}). The average pore diameters for SBA-15 were determined based on the adsorption branches of the isotherms using the DFT/Monte Carlo model.

Solid-state nuclear magnetic resonance spectroscopy for ^{13}C and ^{29}Si (CP/MAS NMR) was performed on a Bruker AC300/P spectrometer. ^{13}C CP/MAS spectra were obtained using pulse sequences with 4 ms contact time, an interval between pulses of 1 s and an acquisition time of 0.041 s. ^{29}Si CP/MAS spectra were obtained using pulse sequences with 3 ms contact time, an interval between pulses of 2 s and acquisition time of 0.041 s. For these two measurements, the chemical shifts were calibrated against TMS standards.

The amount of organic groups immobilized onto the SBA-15 surface was calculated based on the carbon and nitrogen contents, determined by means of elemental analyses on a Perkin–Elmer 2400 elemental analyzer.

2.5. Adsorption isotherms

The interaction of the materials SBA-15/$Bipy^+Cl^-$ and SBA-15/$Bipy^{2+}Cl_2^-$ with anionic Cu(II) complexes in ethanol was evaluated by the adsorption isotherms of $CuCl_2$ in this solvent, obtained using the batch method [47].

To obtain the adsorption isotherms, 50.0 mg of each material was placed into flasks containing 50.0 mL of ethanol solutions having different concentrations of $CuCl_2$. The solutions were stirred for 24 h. The amounts of Cu(II) remaining in solution were determined by titration with EDTA, using 1-(2-pyridylazo)-2-naphthol (PAN) as colorimetric indicator at pH 5. The amount of adsorbed copper ions (N_f) can be calculated by the following equation:

$$N_f = \frac{N_i - [CuCl_2] \cdot V}{m}, \quad (1)$$

where N_i is the initial amount of copper in solution (mol), $[CuCl_2]$ is the $CuCl_2$ equilibrium concentration (mol L^{-1}), V is the solution volume (L) and m is the adsorbent material weight (g). With these

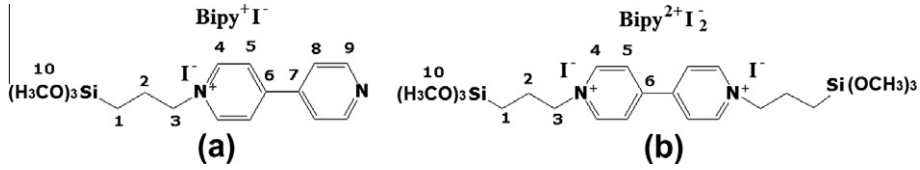

Fig. 1. Structural formula of $Bipy^{+}I^{-}$ and $Bipy^{2+}I_2^{-}$ molecules.

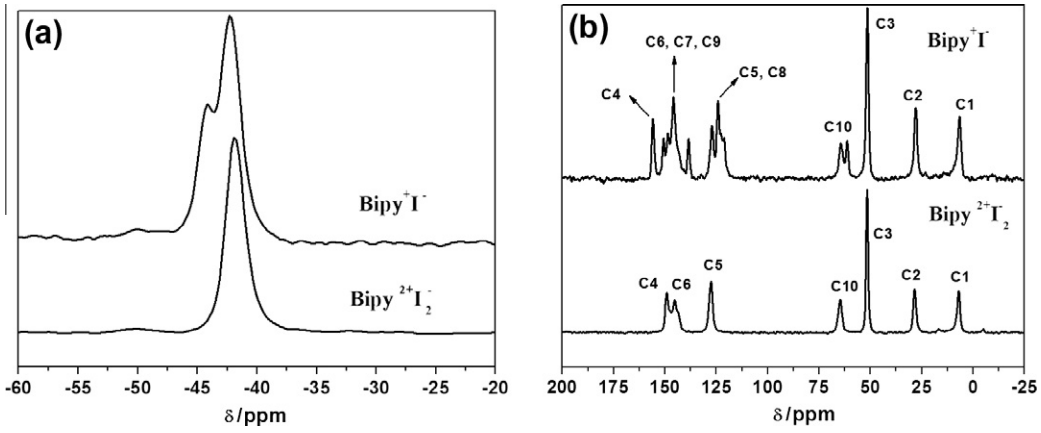

Fig. 2. (a) ^{29}Si and (b) ^{13}C CP/MAS NMR spectra of $Bipy^{+}$ and $Bipy^{2+}$.

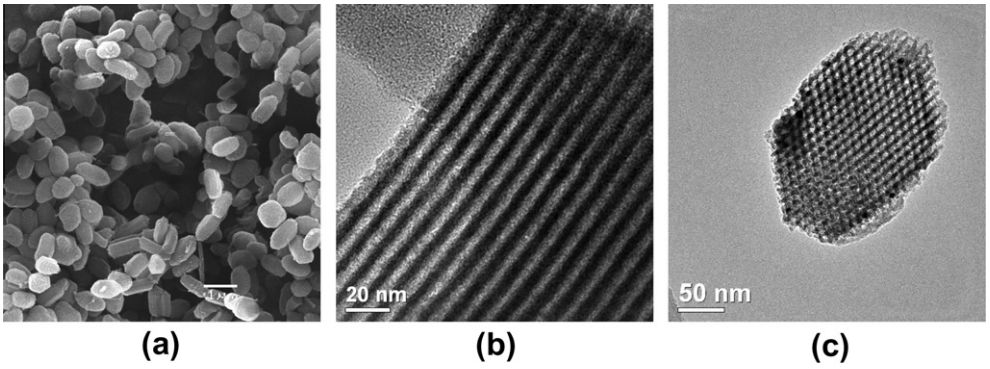

Fig. 3. (a) SEM and (b and c) TEM images of as-prepared SBA-15.

figures, the adsorption isotherm is obtained by plotting the N_f values as functions of $[CuCl_2]$.

3. Results and discussions

3.1. Synthesis and characterization of the materials

Prior to SBA-15 surface functionalization, the C, H, N elemental analyses of the as-prepared functional silylating reagents (a) $Bipy^{+}I^{-}$ ($C_{16}H_{23}N_2SiO_3I$) and (b) $Bipy^{2+}I_2^{-}$ ($C_{22}H_{38}N_2Si_2O_6I_2$) were carried out. The amounts of each element, in wt%, as well as the expected values, in parenthesis, are the following: (a) C = 41.6 (43.1), H = 5.0 (5.2) and N = 5.8 (6.3); (b) C = 35.9 (36.4), H = 4.8 (5.2) and N = 4.0 (3.8). As can be observed, the experimental results are in good agreement with the expected values [46], showing that the mono and disubstituted forms of 4,4′-bipyridine were indeed obtained. Fig. 1 shows the structural formula of both molecules.

The ^{13}C and ^{29}Si CP/MAS NMR spectra were obtained in order to have structural information of the functional molecules (Fig. 2).

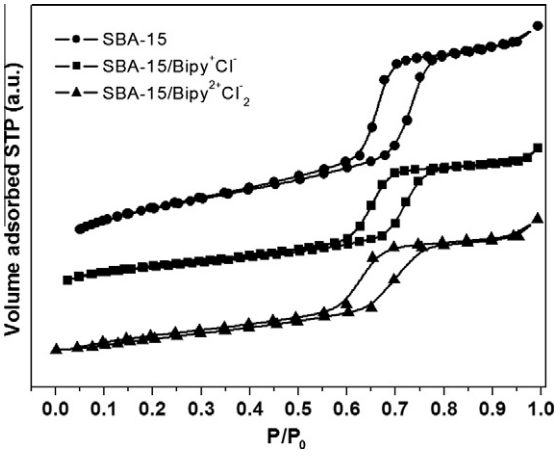

Fig. 4. N_2 adsorption–desorption isotherms of SBA-15 and SBA-15/$Bipy^{n+}Cl_n^{-}$ materials.

Table 1
Specific surface area (S_{BET}), elemental analysis data and functionalization degree of SBA-15 and SBA-15/Bipy^{n+}Cl$_n^-$.

	S_{BET} ($m^2\ g^{-1}$)	N (wt%)	C (wt%)	N_0* (mmol g^{-1})
SBA-15	926	–	–	–
SBA-15/Bipy$^+$Cl$^-$	436	2.02	10.65	0.72
SBA-15/Bipy^{2+}Cl$_2^-$	501	1.56	12.01	0.56

* N_0 = degree of functionalization.

The ^{13}C NMR spectra (Fig. 2b) are in agreement with the expected conformation for Bipy$^+$I$^-$ and Bipy^{2+}I$_2^-$, with peaks assigned according to the numbering showed in Fig. 1 [46]. The ^{29}Si NMR spectra of Bipy^{2+}I$_2^-$ (Fig. 2a) show one peak at −42 ppm, indicating the presence of Si atoms in only one type of chemical environment. This information confirms that the methoxy groups (Si–OCH_3) are not condensed. However, two peaks at −42 and −44 ppm are observed in the ^{29}Si NMR spectra of Bipy$^+$I$^-$, which is an evidence that the methoxy groups can be partially condensed [48].

The morphology and the porous structure features of the synthesized SBA-15 can be observed in Fig. 3, where it is possible to note (Fig. 3a) that it is constituted of micrometer-sized particles (length and width), presenting well-ordered porous structures characterized by uniform cylindrical mesochannels (Fig. 3b and c), with parallel orientation throughout the particle.

The nitrogen adsorption–desorption isotherms for SBA-15, SBA-15/Bipy$^+$Cl$^-$, and SBA-15/Bipy^{2+}Cl$_2^-$ materials are shown in Fig. 4. All of them are type IV isotherms, typical for mesoporous materials, with H1 hysteresis loops, usually associated with porous materials with well-defined cylindrical pore channels and high degrees of pore size uniformity [49,50].

The effect of surface functionalizations of the porous structure of SBA-15 shows the expected reduction of the specific surface areas (Table 1) of the modified materials, when compared to bare SBA-15, which indicates the attachment of the organic groups onto the mesopores surface. The DFT/Monte Carlo pore size distributions were used to obtain the pore size distribution of SBA-15, with average pore diameter having maxima around 8 nm (80 Å). After surface functionalization, the average pore diameters are 7.3 nm for SBA-15/Bipy$^+$Cl$^-$ and 7.0 nm for SBA-15/Bipy^{2+}Cl$_2^-$.

The amount of functional groups immobilized on each surface is also shown in Table 1. The values indicate a higher N_0 for the monocationic ligand when compared to the bicationic one. It should be highlighted that the functional group Bipy$^+$Cl$^-$ is immobilized on the silica surface through one extremity, while the functional group Bipy^{2+}Cl$_2^-$ is immobilized through both extremities. In addition, the length of each functional group is different (Si-Si length = 1.68 nm for Bipy^{2+}Cl$_2^-$ and Si–N length = 1.18 nm for Bipy$^+$Cl$^-$). Consequently, the organization of the molecules on the surface is different, which can explain the different degree of functionalization obtained, although they were prepared under similar experimental conditions.

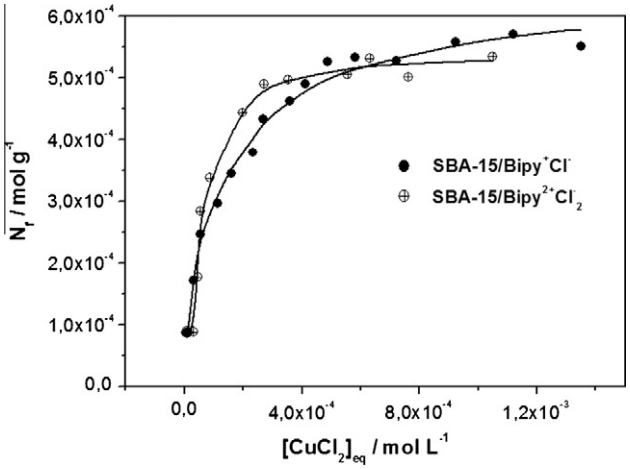

Fig. 6. Experimental (points) and simulated (lines) isotherms of $CuCl_2$ adsorption on SBA-15/Bipy$^+$Cl$^-$ (●) and SBA-15/Bipy^{2+}Cl$_2^-$ (⊕).

In order to have structural information about the functional molecules bonded to the surfaces, ^{13}C and ^{29}Si CP/MAS NMR spectra of SBA-15 and the modified samples were acquired (Fig. 5a and b).

Q units are attributed to Si atoms of the inorganic silica framework in the siloxane binding environment without hydroxyl groups [Q^4 = **Si**$(OSi)_4$], isolated silanol group [Q^3 = **Si**$(OSi)_3OH$] and to geminal silanol groups [Q^2 = **Si**$(OSi)_2(OH)_2$]. T species refer to Si atoms bonded to C atoms of the *n*-propyl bridge of the Bipy^{n+} functional groups [51,52]. The absence of the peak at −42 ppm on the ^{29}Si CP/MAS NMR spectrum of SBA-15/Bipy^{2+}Cl$_2^-$ confirms that the Bipy^{2+}Cl$_2^-$ molecules are immobilized on the silica surface through both extremities. Fig. 5b shows the ^{13}C CP/MAS NMR spectra for both functionalized silicas, SBA-15/Bipy$^+$Cl$^-$ and SBA-15/Bipy^{2+}Cl$_2^-$, with specific peaks positions assigned according to the numbering shown in Fig. 1 [46].

3.2. Adsorption isotherms of $CuCl_2$

The interaction of the resulting materials (SBA-15/Bipy$^+$Cl$^-$ and SBA-15/Bipy^{2+}Cl$_2^-$) with anionic Cu(II) chloride in ethanol was evaluated by adsorption isotherms, shown in Fig. 6.

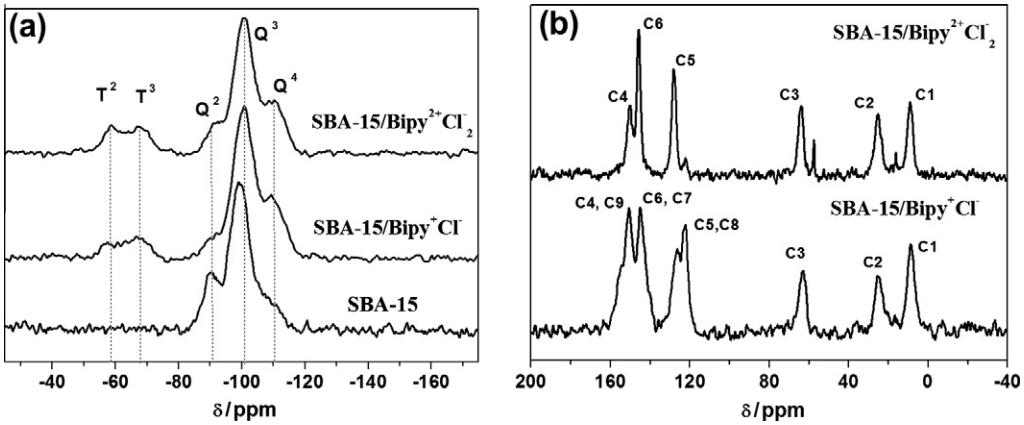

Fig. 5. (a) ^{29}Si and (b) ^{13}C CP/MAS NMR spectra for SBA-15 and SBA-15/Bipy^{n+}Cl$_n^-$ materials.

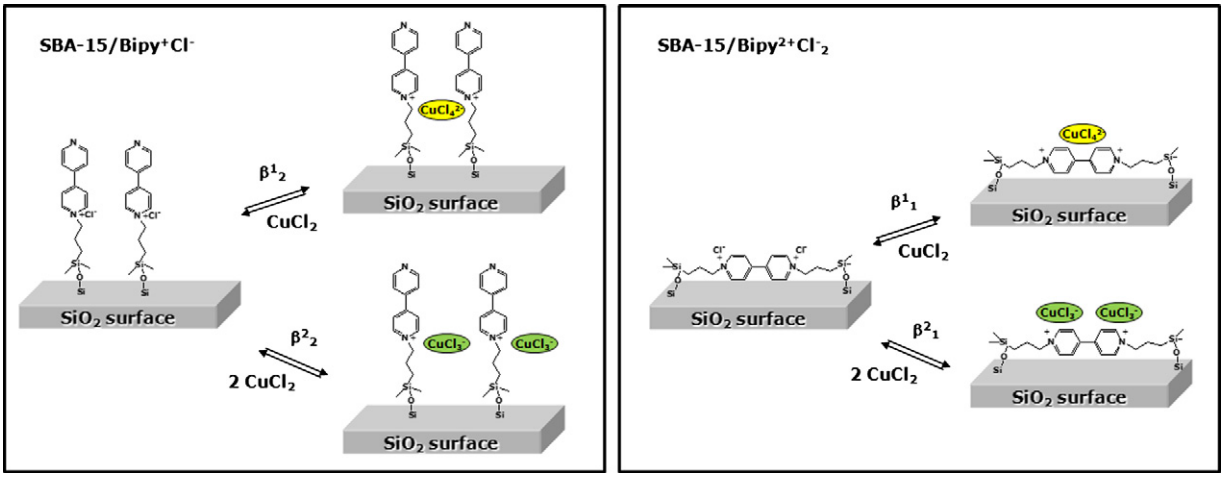

Fig. 7. Schematic representation of $CuCl_2$ adsorption equilibrium. Formation of $CuCl_4^{2-}$ and $CuCl_3^-$ complexes on the SBA-15/Bipy^{n+} surface.

Table 2
Parameters obtained for $CuCl_2$ adsorption from anhydrous ethanol at 298 K.

	$\log \beta_j^1$	$\log \beta_j^2$	t_Q (mmol g^{-1})	N_0 (mmol g^{-1})
SBA-15/Bipy$^+$Cl$^-$	4.42 (±0.07)	7.79 (±0.06)	0.67	0.72
SBA-15/Bipy^{2+}Cl$_2^-$	3.75 (±0.10)	8.37 (±0.08)	0.53	0.56
DMS/Bipy$^+$Cl$^-$	4.02 (±0.13)	7.95 (±0.08)	0.51	0.61
DMS/Bipy^{2+}Cl$_2^-$	3.77 (±0.07)	7.67 (±0.05)	0.54	0.78

The $CuCl_2$ adsorption process occurs at the solid–solution interface through the formation of anionic copper-chloride complexes ($CuCl_4^{2-}$ and $CuCl_3^-$) that act as counter-ions of the Bipy$^+$ and Bipy^{2+} groups. Fig. 7 shows the reactions that describe the adsorption process on the surface of the materials. Using this model, the respective stability constants can be determined and are represented by β_j^i, where the subscript refers to the number of functional groups per adsorption center, and the superscript is assigned as the order of the constant. According to the model proposed, one adsorption center comprises two positively charged nitrogen atoms. Therefore, in the case of SBA-15/Bipy$^+$Cl$^-$, two functional groups must be considered to generate one adsorption center ($j = 2$), and in the case of SBA-15/Bipy^{2+}Cl$_2^-$, one functional group forms one adsorption center ($j = 1$).

The schematic representation of $CuCl_2$ adsorption equilibrium is based on our knowledge that the anionic species $CuCl_4^{2-}$ and $CuCl_3^-$ are very stable in anhydrous ethanol with the formation stability constants $\log(CuCl_3^-) = 7.8$ and $\log(CuCl_4^{2-}) = 8.3$ [53]. Therefore, as illustrated in Fig. 7, when $CuCl_2$ diffuse into the solid–solution interface, the transfer of the counter-ion Cl$^-$ of SBA-15/Bipy$^+$Cl$^-$ or SBA-15/Bipy^{2+}Cl$^-$ to the coordination sphere of $CuCl_2$ forming the $CuCl_{2+n}^{n-}$ species is favored. The anionic complex species are retained on the surface by an ionic electrostatic interaction.

All calculations for this model were performed with CLINP 2.1 software program [54,55]. The program has allowed to calculate the constants of adsorption equilibria and to estimate the degrees of formation of different species on the surface [56–58]. The parameters for fitting obtained for each material are presented in Table 2. All these values, $\log \beta_j^i$ (stability constants) and t_Q (effective adsorption capacity), were taken from the calculated isotherms curves (lines) in Fig. 6 while N_0 is the experimentally determined degree of functionalization (Table 1). For comparison, Table 2 also shows the results obtained for a non-ordered mesoporous silica modified with both functional groups, designated as DMS/Bipy$^+$Cl$^-$ and DMS/Bipy^{2+}Cl$_2^-$ (DMS = disordered mesoporous silica) [Supplementary material].

It can be seen from the results that the amount of copper ions adsorbed is higher for SBA-15/Bipy$^+$Cl$^-$, due to the higher functionalization degree presented by this material. For both materials, the ratio between organic molecules and adsorbed copper ions is

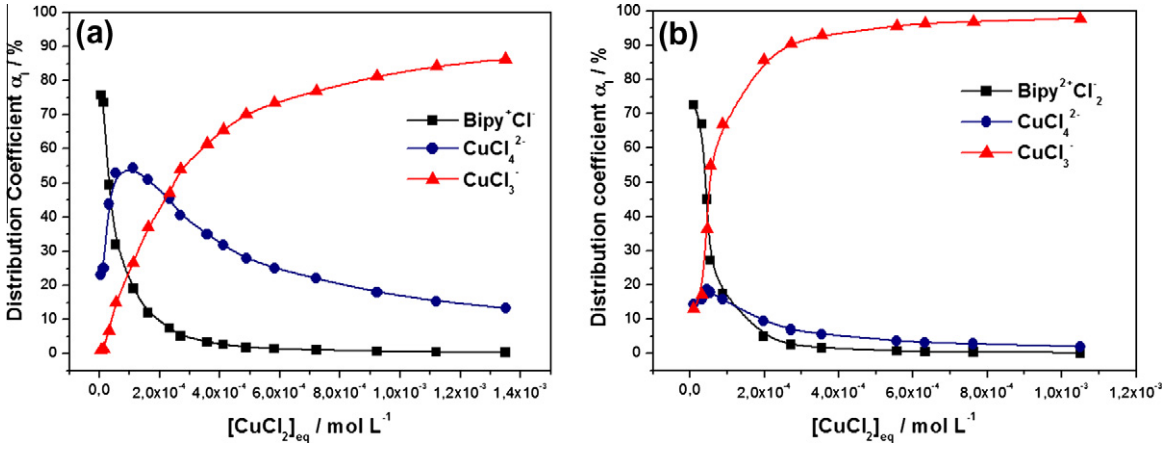

Fig. 8. Plots of distribution coefficients, α_i, of species $CuCl_4^{2-}$, $CuCl_3^-$ and Bipy^{n+} versus $CuCl_2$ concentrations in ethanol solution for (a) SBA-15/Bipy$^+$Cl$^-$ and (b) SBA-15/Bipy^{2+}Cl$_2^-$

approximately 1:1, which means an exchange efficiency (defined as $\varepsilon = t_Q \times 100/N_0$) of 93% for SBA-15/Bipy$^+Cl^-$ and 94% for SBA-15/Bipy^{2+}Cl$_2^-$, due to the homogeneous distribution of functional groups throughout the surface of the porous substrate.

For comparison, results obtained for DMS/Bipy$^+$Cl$^-$ and DMS/Bipy^{2+}Cl$_2^-$ showed that the efficiency of $CuCl_2$ interacting with the adsorbent is considerably reduced: $\varepsilon = 83\%$ for DMS/Bipy$^+$Cl$^-$ and $\varepsilon = 69\%$ for DMS/Bipy^{2+}Cl$_2^-$. Although the stability constants are nearly the same order (Table 2), the observed differences of exchange efficiency are due to the heterogeneous nature of the surface in the DMS matrix. In this matrix, the pore size distribution is not uniform and many of the functional groups are presumably not accessible to the copper chloride [43].

The distribution coefficient, α_i, of $CuCl_4^{2-}$ and $CuCl_3^-$ on the solid surface was calculated as:

$$\alpha_i = \frac{\{i\}}{\{CuCl_4^{2-}\} + \{CuCl_3^-\} + \{Bipy^n + Cl_n^-\}} \quad (2)$$

where $\{i\}$ is the individual concentration of the species $\{CuCl_4^{2-}\}$, $\{CuCl_3^-\}$ or $\{Bipy^{n+}Cl_2^-\}$ on the surface. Fig. 8 shows the correlation between the distribution coefficients α_i and the $CuCl_2$ equilibrium concentrations. The calculated values of α_i indicate that the formation of $CuCl_3^-$ species predominates for both materials.

4. Conclusions

SBA-15 chemically modified by post-grafting with 4,4′-bipyridine alkoxysilane derivatives successfully produced SBA-15 Bipy$^+$Cl$^-$ and SBA-15/Bipy^{2+}Cl$_2^-$, which showed efficiency in adsorbing $CuCl_2$, used as a probe in the present work, due to the ordered attachment of these functional groups on the surface of the matrix's channel. The ability of controlling the homogeneity and the dispersion degree of the functional groups on the substrate surface is very important since it results in materials with the active sites uniformly spaced and well-oriented on the surface, with optimized hosting and recognition properties, which is essential for applications as adsorbent materials.

Acknowledgments

NF is indebted to FAPESP for a Master's fellowship (Grant 2009/12189-5). CMM is indebted to CNPq for a postdoctoral fellowship. YK is indebted to the Ministry of Education and Science, Youth and Sport of Ukraine for financial support (project 0110U001453). YG is indebted to CNPq and FAPESP for financial support and to Prof. C.H. Collins for English revision. Contributions from LNNano-LME (Campinas-SP, Brazil) for TEM analyses are also gratefully acknowledged.

Appendix A. Supplementary material

Supplementary data associated with this article can be found, in the online version, at http://dx.doi.org/10.1016/j.jcis.2012.06.065.

References

[1] F.Z. El Berrichi, C. Pham-Huu, L. Cherif, B. Louis, M.J. Ledoux, Catal. Commun. 12 (2011) 790.
[2] H. Li, R. Wang, Q. Hong, L. Chen, Z. Zhong, Y. Koltypin, J. Calderon-Moreno, A. Gedanken, Langmuir 20 (2004) 8352.
[3] Y. Guo, C. Hu, C. Jiang, Y. Yang, S. Jiang, X. Li, E. Wang, J. Catal. 217 (2003) 141.
[4] A. Citak, B. Erdem, S. Erdem, R.M. Oksuzoglu, J. Colloid Interface Sci. 369 (2012) 160.
[5] C. Lei, Y. Shin, J. Liu, E.J. Ackerman, J. Am. Chem. Soc. 124 (2002) 11242.
[6] A. Salis, D. Meloni, S. Ligas, M.F. Casula, M. Monduzzi, V. Solinas, E. Dumitriu, Langmuir 21 (2005) 5511.
[7] A. Nieto, M. Colilla, F. Balas, M. Vallet-Regi, Langmuir 26 (2010) 5038.
[8] X. Zhang, S. Duan, X. Xu, S. Xu, C. Zhou, Electrochim. Acta 56 (2011) 1981.
[9] C.H. Hung, K.P. Chang, H.D. Ou, Y.C. Chiang, C.F. Wang, Microporous Mesoporous Mater. 141 (2011) 102.
[10] Y. Dong, B. Lu, S. Zang, J. Zhao, X. Wang, Q. Cai, J. Chem. Technol. Biotechnol. 86 (2011) 616.
[11] H. Vinh-Thang, Q. Huang, M. Eic, D. Trong-On, S. Kaliaguine, Langmuir 21 (2005) 5094.
[12] R.M. Rioux, J.D. Hoefelmeyer, M. Grass, H. Song, K. Niesz, P. Yang, G.A. Somorjai, Langmuir 24 (2008) 198.
[13] X. Feng, G.E. Fryxell, L.Q. Wang, A.Y. Kim, J. Liu, K.M. Kemner, Science 276 (1997) 923.
[14] R.I. Nooney, M. Kalyanaraman, G. Kennedy, E.J. Maginn, Langmuir 17 (2001) 528.
[15] H. Yoshitake, J. Mater. Chem. 20 (2010) 4537.
[16] H. Ghassabzadeh, A. Mohadespour, M. Torab-Mostaedi, P. Zaheri, M.G. Maragheh, H. Taheri, J. Hazard. Mater. 177 (2010) 950.
[17] M. Najafia, R. Rostamian, A.A. Rafati, Chem. Eng. J. 168 (2011) 426.
[18] C. McManamon, A.M. Burke, J.D. Holmes, M.A. Morris, J. Colloid Interface Sci. 369 (2012) 330.
[19] L. Mercier, T. Pinnavaia, J. Environ. Sci. Technol. 32 (1998) 2749.
[20] S. Fiorilli, D. Caldarola, H. Ma, B. Onida, J. Sol–Gel Sci. Technol. 60 (2011) 260.
[21] X. Sheng, J. Gao, L. Han, Y. Jia, W. Sheng, Microporous Mesoporous Mater. 143 (2011) 73.
[22] Y.-S. Jun, Y.S. Huh, H.S. Park, A. Thomas, S.J. Jeon, E.Z. Lee, H.J. Won, W.H. Hong, S.Y. Lee, Y.K. Hong, J. Phys. Chem. C 111 (2007) 13076.
[23] H. Yang, K. Zheng, Z. Zhang, W. Shi, S. Jing, L. Wang, W. Zheng, D. Zhao, J. Xu, P. Zhang, J. Colloid Interface Sci. 369 (2012) 317.
[24] M. Álvaro, G.A. Facey, H. García, S. García, J.C. Scaiano, J. Phys. Chem. 100 (1996) 18173.
[25] E.L. Clennan, Coord. Chem. Rev. 248 (2004) 477.
[26] P.M.S. Monk, The Viologens, Physicochemical Properties, Synthesis and Applications of the Salts of 4,4′-bipyridine, Wiley, Chichester, UK, 1998.
[27] T. Sata, J. Membr. Sci. 118 (1996) 121.
[28] T. Kinuta, T. Sato, N. Tajima, R. Kuroda, Y. Matsubara, J. Mol. Struct. 982 (2010) 45.
[29] H. Li, F. Li, C. Han, Z. Cui, G. Xie, A. Zhang, Sens. Actuators, B 145 (2010) 194.
[30] M. Ohashi, M. Aoki, K. Yamanaka, K. Nakajima, T. Ohsuna, T. Tani, S. Inagaki, Chem. Eur. J. 15 (2009) 13041.
[31] K. Maruszewski, A. Hreniak, J. Czyzzewski, W. Strezk, Opt. Mater. 22 (2003) 221.
[32] A. Liu, S. Han, H. Che, L. Hua, Langmuir 26 (2010) 3555.
[33] W. Cao, H. Zhang, Y. Yuan, Catal. Lett. 91 (2003) 243.
[34] P. Yang, Y. Cao, J.-C. Hu, W.-L. Dai, K.-N. Fan, Appl. Catal., A 241 (2003) 363.
[35] Y.N. Belokon, W. Clegg, R.W. Harrington, M. North, C. Young, Inorg. Chem. 47 (2008) 3801.
[36] P.D. Benny, G.A. Fugate, A.O. Barden, J.E. Morley, E. Silva-Lopez, B. Twamley, Inorg. Chem. 47 (2008) 2240.
[37] C.-M. Yang, P.-H. Liu, Y.-F. Ho, C.-Y. Chiu, K.-J. Chao, Chem. Mater. 15 (2003) 275.
[38] C.-M. Yang, M. Kalwei, F. Schüth, K.-J. Chao, Appl. Catal., A 254 (2003) 289.
[39] W.-T. Chen, D.-S. Liu, S.-M. Ying, H.-L. Chen, Y.-P. Xu, Inorg. Chem. Commun. 11 (2008) 1212.
[40] M.S. Iamamoto, Y. Gushikem, Analyst 114 (1989) 983.
[41] S.T. Fujiwara, Y. Gushikem, R.V.S. Alfaya, Colloids Surf., A 178 (2001) 135.
[42] R.V.S. Alfaya, S.T. Fujiwara, Y. Gushikem, Y.V. Kholin, J. Colloid Interface Sci. 269 (2004) 32.
[43] C.M. Maroneze, H.A. Magosso, A.V. Panteleimonov, Y.V. Kholin, Y. Gushikem, J. Colloid Interface Sci. 356 (2011) 248.
[44] D. Zhao, Q. Huo, J. Feng, B.F. Chmelka, G.D. Stucky, J. Am. Chem. Soc. 120 (1998) 6024.
[45] D. Zhao, J. Feng, Q. Huo, N. Melosh, G.H. Fredrickson, B.F. Chmelka, G.D. Stucky, Science 279 (1998) 548.
[46] M. Álvaro, B. Ferreira, V. Fornés, H. García, Chem. Commun. (2001) 2546.
[47] H.A. Magosso, N. Fattori, Y.V. Kholin, Y. Gushikem, J. Braz. Chem. Soc. 20 (2009) 744.
[48] S.A. Torry, A. Campbell, A.V. Cunliffe, D.A. Tod, Int. J. Adhes. Adhes. 26 (2006) 40.
[49] M. Kruk, M. Jaroniec, Chem. Mater. 13 (2001) 3169.
[50] K.S.W. Sing, D.H. Everett, R.A.W. Haul, L. Moscou, R.A. Pierotti, J. Rouquerol, T. Siemieniewska, Pure Appl. Chem. 57 (1985) 603.
[51] L.T. Arenas, A.C. Pinheiro, J.D. Ferreira, P.R. Livotto, V.P. Pereira, M.R. Gallas, Y. Gushikem, T.M.H. Costa, E.V. Benvenutti, J. Colloid Interface Sci. 318 (2008) 96.
[52] X. Rios, P. Moriones, J.C. Echeverria, A. Luquin, M. Laguna, J. Garrido, Adsorption 17 (2011) 583.
[53] S. Chafaa, T. Douadi, M.A. Khan, J. Meullemeestre, M.J. Schwing, F. Vierling, Nouveau J. Chim. 15 (1991) 39.
[54] S.A. Merny, D.S. Konyaev, Y.V. Kholin, Kharkov Univ. Bull. 420 (1998) 112.
[55] <http://www-chemo.univer.kharkov.ua/kholin/clinp.html> (accessed on 16.04.12).
[56] F.L. Pissetti, H.A. Magosso, I.V.P. Yoshida, Y. Gushikem, S.O. Myernyi, Y.V. Kholin, J. Colloid Interface Sci. 38 (2007) 38.
[57] A.M.S. Lucho, A.V. Panteleimonov, Y.V. Kholin, Y. Gushikem, J. Colloid Interface Sci. 310 (2007) 47.
[58] H.A. Magosso, A.V. Panteleimonov, Y.V. Kholin, Y. Gushikem, J. Colloid Interface Sci. 303 (2006) 18.